rf-SQUID-Mediated Coherent Tunable Coupling between a Superconducting Phase Qubit and a Lumped-Element Resonator

M. S. Allman, F. Altomare, J. D. Whittaker, K. Cicak, D. Li, A. Sirois, J. Strong, J. D. Teufel, and R. W. Simmonds*

National Institute of Standards and Technology, 325 Broadway, Boulder, Colorado 80305-3328, USA

(Received 6 January 2010; published 29 April 2010)

We demonstrate coherent tunable coupling between a superconducting phase qubit and a lumped-element resonator. The coupling strength is mediated by a flux-biased rf SQUID operated in the nonhysteretic regime. By tuning the applied flux bias to the rf SQUID we change the effective mutual inductance, and thus the coupling energy, between the phase qubit and resonator. We verify the modulation of coupling strength from 0 to 100 MHz by observing modulation in the size of the splitting in the phase qubit's spectroscopy, as well as coherently by observing modulation in the vacuum Rabi oscillation frequency when on resonance. The measured spectroscopic splittings and vacuum Rabi oscillations agree well with theoretical predictions.

DOI: 10.1103/PhysRevLett.104.177004 PACS numbers: 85.25.Dq, 42.50.Pq, 85.25.Cp, 85.25.Hv

Superconducting qubit research has made tremendous strides in recent years [1]. A number of coupled qubit experiments with fixed coupling between qubits have been performed [2–9]. Any real superconducting quantum computer, however, will be composed of an intricate network of many qubits coupled to each other in various ways. Coherent "quantum buses" will manage the shuttling of quantum information between distant qubits. It will become increasingly difficult to implement quantum information processing between many coupled quantum circuits with fixed coupling between elements. The need to control the coupling between various elements, such as qubit-qubit interactions or qubit-quantum bus interactions, is essential. A number of ways of implementing tunable coupling have been proposed in recent years [10–14] and performed experimentally [15–19]. One rather conceptually simple way of implementing tunable coupling, proposed by [14], involves use of a flux-biased rf SQUID, operated in the nonhysteretic regime, as a tunable "flux transformer" between elements. We have employed such a coupling scheme to coherently couple a superconducting phase qubit to a lumped-element resonator.

The circuit for this experiment is illustrated in Fig. 1. It is composed of a phase qubit, with Josephson inductance $L_{Jq} = \Phi_0/2\pi I_{q0}$, where $\Phi_0 = h/2e$ is the magnetic flux quantum and I_{q0} is the junction critical current, geometric inductance L_q, capacitance $C_q = C_s + C_{Jq}$, where C_s is a shunt capacitor and C_{Jq} is the junction capacitance, coupled through a mutual inductance M_{qc}, to the rf SQUID, referred to as "the coupler." The coupler has a Josephson inductance L_{Jc}, geometric inductance L_c, and junction capacitance C_{Jc}. It is coupled through a mutual inductance M_{cr} to the lumped-element resonator of geometric inductance L_r and capacitance C_r. All the junctions are via-style ion-mill junctions, and the capacitors were fabricated by use of "vacuum" capacitor technology [20]. There is also a residual mutual inductance M_{qr} between the qubit and resonator, which was gradiometrically designed to be as small as possible.

A dc bias line, coupled to the qubit loop via a mutual inductance M_{qb}, provides an external flux bias to the qubit. This bias changes the nonlinear Josephson inductance of the qubit and controls the energy level spacing between qubit states as well as level anharmonicity. The qubit is operated in a flux bias regime that creates an approximately cubic metastable potential well of sufficient anharmonicity to reliably isolate the lowest two energy states of the well [21].

A microwave drive capacitively coupled via the series capacitance C_x provides the excitation energy to drive transitions between the two lowest qubit levels, labeled $|g\rangle$ and $|e\rangle$, respectively. On the dc bias line, a short ($\sim$5 ns), capacitively coupled measure pulse [22] induces the tunneling of the $|e\rangle$ state to the adjacent stable well. The occupation probability of the qubit excited state P_e is read

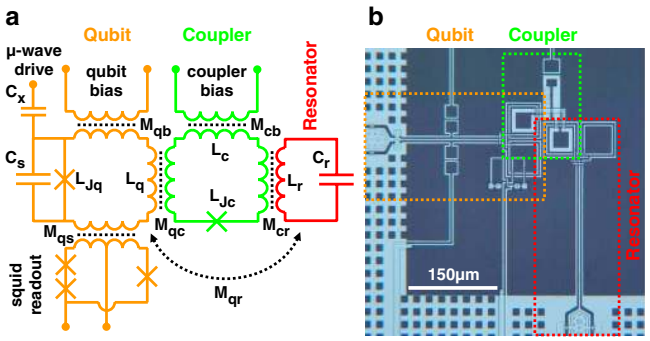

FIG. 1 (color online). (a) Circuit diagram for the phase qubit, coupler, and resonator. The qubit parameters are $L_{Jq} \simeq 550$ pH, $I_{q0} \simeq 0.6$ μA, $L_q \simeq 1000$ pH, $C_s \simeq 0.6$ pF, $C_{Jq} \simeq 0.3$ pF, and $M_{qc} \simeq 60$ pH. The coupler parameters are $L_{Jc} \simeq 370$ pH, $I_{c0} \simeq 0.9$ μA, $L_c \simeq 200$ pH, and $C_{Jc} \simeq 0.3$ pF. The resonator parameters are $L_r \simeq 1000$ pH, $C_r \simeq 0.4$ pF, and $M_{cr} \simeq 60$ pH. (b) Optical micrograph of the circuit.

out via a dc SQUID coupled to the qubit's geometric inductance via a mutual inductance M_{qs} [21,22].

The qubit's circulating current I_q couples an amount of flux $M_{qc}I_q$ into the coupler, generating a circulating current I_c governed by the relation

$$i_c = -\sin(2\pi\phi_x + \beta_c i_c), \tag{1}$$

where $i_c = I_c/I_{c0}$ is the normalized circulating coupler current, $\phi_x = (\Phi_x + M_{qc}I_q)/\Phi_0$ is the net external flux applied to the coupler, and $\beta_c = 2\pi L_c I_{c0}/\Phi_0 < 1$. This current then couples flux to the resonator via mutual inductance M_{cr}. For a given change in qubit flux, the flux change seen by the resonator depends on the offset current circulating in the coupler due to the external bias flux Φ_x. The result is a tunable effective mutual inductance between the qubit and resonator given by

$$M_{\text{eff}}(\Phi_x) = M_{qc}M_{cr}\frac{I_{c0}}{\Phi_0}\frac{\partial i_c}{\partial \phi_x} = -\frac{M_{qc}M_{cr}}{L_c}\frac{\beta_c\cos[2\pi\phi_x + \beta_c i_c]}{(1 + \beta_c\cos[2\pi\phi_x + \beta_c i_c])}. \tag{2}$$

From Eq. (2) we see that the effective mutual inductance can be tuned anywhere between the following extrema:

$$(M_{\text{eff}})_{\max} = \frac{M_{qc}M_{cr}}{L_c}\frac{\beta_c}{1-\beta_c} \quad \text{for } n_{\text{odd}}, \tag{3}$$

$$(M_{\text{eff}})_{\min} = -\frac{M_{qc}M_{cr}}{L_c}\frac{\beta_c}{1+\beta_c} \quad \text{for } n_{\text{even}}, \tag{4}$$

by choosing Φ_x such that

$$\Phi_x = n\frac{\Phi_0}{2} - M_{qc}I_q, \tag{5}$$

corresponding to a null circulating current in the coupler. In particular, $M_{\text{eff}} = 0$, when the coupler circulating current is at the critical current. It is also worth noting that in the limit that $\beta_c \to 1$, $(M_{\text{eff}})_{\max}$ increases without bound.

An interesting consequence of the changing effective mutual inductance between the qubit and resonator is that the resonator's frequency modulates with the applied flux as

$$\omega_r(\Phi_x) = \omega_{r0}\sqrt{1 - \frac{M_{cr}}{L_r M_{qc}}M_{\text{eff}}(\Phi_x)}, \tag{6}$$

where $\omega_{r0} = 1/\sqrt{L_r C_r}$. The measured resonator frequency is shown in Fig. 2(b).

We approximate the Hamiltonian of our system using the Jaynes-Cummings model in the rotating-wave approximation,

$$\hat{H} = \hat{H}_q + \hat{H}_r + \hat{H}_I(\Phi_x) + \hat{H}_\kappa + \hat{H}_\gamma, \tag{7}$$

where $\hat{H}_q = \frac{1}{2}\hbar\omega_q\hat{\sigma}_{qz}$ is the qubit Hamiltonian, $\hat{H}_r = (\hat{a}_r\hat{a}_r^\dagger + \frac{1}{2})\hbar\omega_r$ is the resonator Hamiltonian, and the interaction term, $\hat{H}_I(\Phi_x) = \hbar g_c(\Phi_x)(\hat{\sigma}_q^+\hat{a}_r + \hat{\sigma}_q^-\hat{a}_r^\dagger)$, describes the exchange of a single excitation between the qubit and resonator at a rate proportional to

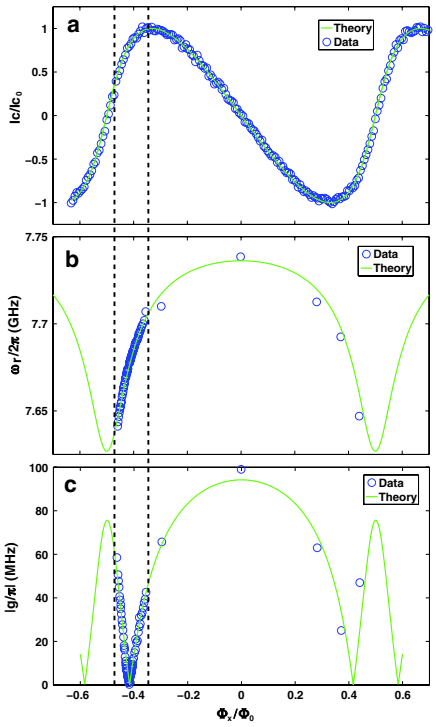

FIG. 2 (color online). Measured dependence of I_c, ω_r, and g_c on applied coupler flux, Φ_x/Φ_0. The vertical dashed lines bracket the applied flux ranges for the waterfall data shown in Fig. 3. (a) The measured circulating coupler current as a function of applied coupler flux along with the theoretical fit giving $\beta_c = 0.51$. (b) Measured resonator frequency as a function of applied coupler flux, along with theoretical fit using β_c extracted from (a). The fit yields $\omega_{r0}/2\pi = 7.710$ GHz. (c) Measured coupling strength as a function of applied coupler flux along with the theoretical fit using parameters extracted from the theory fits in (a) and (b). Note that the position of zero coupling does not coincide with the coupler biased at its critical current. This is due to a cancelable direct coupling ($g_0 \sim 50$ MHz) between the qubit and resonator resulting from their close proximity.

$$g_c(\Phi_x) \simeq \frac{\omega_r}{2}\frac{M_{\text{eff}}(\Phi_x)}{\sqrt{L_q L_r}} + g_0, \tag{8}$$

where g_0 incorporates any direct coupling between the qubit and resonator [23]. The last two terms, H_κ and H_γ, describe the coupling of the resonator and qubit to environments that give rise to the resonator decay rate κ and qubit decay rate γ [24].

We label the qubit's ground and first excited states as $|g\rangle$ and $|e\rangle$, respectively, and the resonator's ground and first excited states as $|0\rangle$ and $|1\rangle$, respectively. According to Eq. (7), when the qubit is on resonance with the resonator, so that the detuning $\Delta = \omega_q - \omega_r = 0$, individual eigenstates of the qubit and resonator, given by $|g0\rangle$, $|e0\rangle$, $|g1\rangle$, and $|e1\rangle$ are no longer the eigenstates of the coupled system. The new eigenstates are found to be $|g0\rangle$ and $|e1\rangle$ and the symmetric and antisymmetric superpositions $|\pm\rangle = (|g1\rangle \pm |e0\rangle)/\sqrt{2}$. The corresponding energy eigen-

values are $E_{g0} = 0$, $E_{e1} = 2\hbar\omega_r$, and $E_{\pm} = \hbar[\omega_r \pm g_c(\Phi_x)]$.

The coupler is first calibrated by sweeping its external flux bias Φ_x and measuring the effect on the tunneling probability of the $|g\rangle$ state of the qubit. By tracking the required applied qubit flux Φ_q, to maintain a constant total qubit flux $\phi_q = (\Phi_q + M_{qc}I_c)/\Phi_0$ such that the $|g\rangle$ state tunneling probability is approximately 10%, we can determine the circulating current in the coupler as a function of Φ_x. Figure 2(a) shows the measured coupler circulating current as a function of applied coupler bias flux.

Next we demonstrate the effect of the coupler on the quantum mechanical interactions between the qubit and cavity. We look for interactions using well-established spectroscopic techniques [21,22]. Qubit spectroscopic measurements are performed for different coupler fluxes. When the qubit transition frequency nears the resonant frequency of the resonator, an avoided crossing occurs, splitting the resonant peak into two peaks. When the qubit frequency exactly matches the resonator's frequency ($\Delta = 0$), the separation of the spectroscopic peaks is minimized to the vacuum Rabi splitting size $g(\Phi_x)/\pi$. This whole cycle is repeated for different flux biases applied to the coupler. We observe the size of the zero-detuning splitting modulate from a maximum of $g_{\max}/\pi \approx 100$ MHz down to no splitting [Fig. 3(a)]. The spectroscopic measurements are a good indicator that the coupler is working, but we do not consider them to be proof of coherent coupling between the qubit and resonator, because the length of the microwave pulse is longer ($\simeq$500 ns) than the lifetime of the qubit.

To demonstrate coherent tunable coupling we perform time-domain measurements to acquire the vacuum Rabi oscillation period between the qubit and resonator as a function of applied coupler flux. According to Eq. (7), neglecting dissipation, the zero-detuning probability of finding the system in the state $|e0\rangle$ as a function of time is periodic and given by

$$|\langle e0|\Psi(t)\rangle|^2 = |\langle e0|e^{i\hat{H}t/\hbar}|e0\rangle|^2 = \frac{1}{2}(1 + \cos(2g_c(\Phi_x)t)). \tag{9}$$

When dissipation is added the oscillatory behavior of Eq. (9) decays exponentially with a rate given by $\gamma_{\rm av} = (\gamma + \kappa)/2$. When $|4g(\Phi_x)| = |\kappa - \gamma|$, the system is critically damped and the $|e0\rangle$ state decays at the rate $\gamma_{\rm av}$ with no oscillations [25]. The qubit's decay rate was measured to be $\gamma = 1/T_1 = 1/135$ ns. The resonator's decay rate was not measured in this experiment directly, but previous experiments have found them to be smaller than $\kappa \sim 1/1000$ ns [20]. If we take $\gamma \gg \kappa$, then the critical coupling strength where the oscillations are expected to disappear is $g_c/\pi \simeq 1$ MHz.

Experimentally, we excite the qubit to prepare the $|e0\rangle$ state by applying a short microwave π pulse (5–10 ns) with the qubit on resonance with the resonator. The pulse is short enough that the resonator remains in its ground state during state preparation. We then measure the state of the qubit as a function of time. Figures 2(b), 2(c), and 3 summarize the spectroscopic and time-domain measurements. For $g(\Phi_x)/\pi > 10$ MHz, the vacuum Rabi data are used to determine the coupling strength by applying a fast Fourier transform (FFT) to the measured probability data. For $g(\Phi_x)/\pi < 10$ MHz, the FFT method is less reliable and the coupling strength is determined from the size of the splitting in the spectroscopy data at zero detuning. We clearly see the splitting in the spectroscopy shrink to zero when the coupler is "off," but the corresponding time-domain data do not appear to be exponential, as predicted by Eq. (7) when $g_c(\Phi_x) = 0$. There appears to be a rapid drop followed by a slow ($\simeq$7 MHz), low amplitude oscillation in the data (Fig. 4).

There is a higher order coupling channel not included in Eq. (8), resulting from the finite but small direct mutual inductance between the qubit and resonator, M_{qr}. This residual coupling strength is given by Eq. (35) in Ref. [26]. For our design parameters $g_{\rm residual} \sim 10$ kHz, much too weak to account for the residual effect seen in the data. We believe that what appears to be a residual coupling effect is due to weakly coupled, spurious two-level system fluctuators (TLSs) interacting with the qubit at this frequency [21,27]. We have made time-domain measurements throughout the qubit's entire spectral range (7–9 GHz) that show weak temporal oscillations, with different beat periods, some more coherent-looking than others, localized at particular qubit frequencies where no coupling was evident in the corresponding spectroscopic measurements. This is likely to be due to the fact that the long spectroscopic pulse durations produce a saturation effect. In clean regions, we find the expected exponential behavior

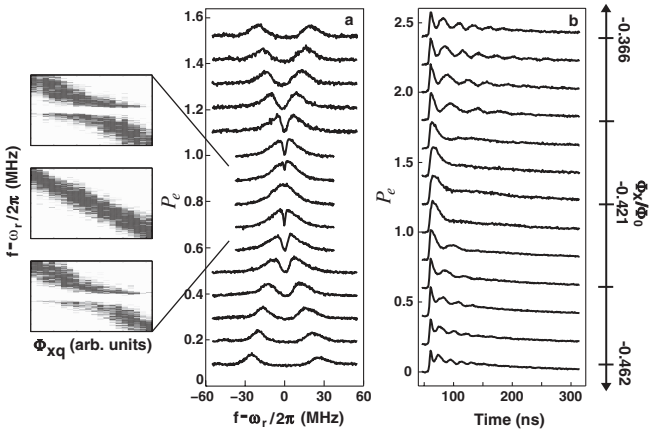

FIG. 3. Spectroscopic and time-domain data over the range $\Phi_x/\Phi_0 = -0.462$ to -0.366. (a) Waterfall plot of the spectroscopic measurements showing the splitting transition from $g_c(-0.462)/\pi \simeq 50$ MHz through $g_c(-0.421)/\pi = 0$ to $g_c(-0.366)/\pi \simeq 40$ MHz. The inset to the left is a 3D plot of the qubit spectroscopy for applied coupler flux values close to $\Phi_x = -0.421$. (b) The corresponding vacuum Rabi measurements demonstrating coherent modulation in the coupling strength $g_c(\Phi_x)$.

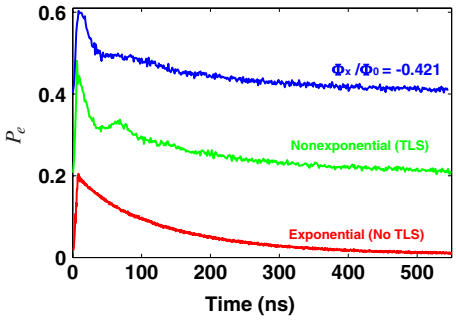

FIG. 4 (color online). A higher resolution trace of the occupation probability of the qubit excited state P_e when $\Phi_x/\Phi_0 = -0.421$ along with other time-domain measurements that show nonexponential and exponential (T_1 decay) behavior when taken at qubit frequencies largely detuned from the resonator. The nonexponential trace shows no evidence of a TLS interaction in the corresponding spectroscopy (not shown).

for energy decay of the qubit. This suggests that traditional spectroscopic measurements may not be sufficient in locating all TLS defects. Indeed, using fine resolution scans of time-domain measurements we detect the additional presence of weakly coupled TLSs [28] as predicted by the standard TLS tunneling model [27]. As an example, we have extracted from these scans exponential versus nonexponential time-domain behavior at two qubit frequencies far detuned from the resonator. Figure 4 compares these curves with the results obtained on resonance with the resonator when the coupler is ''off.''

We have demonstrated coherent tunable coupling between a superconducting phase qubit and a lumped-element resonator, using a separate, flux-biased rf SQUID as a mediating element. The coupling strength was observed to modulate from a maximum 100 MHz to zero.

This work was supported by NIST, the NSA, and by ARO Grant No. W911NF-06-1-0384.

*simmonds@boulder.nist.gov

[1] J. Clarke and F. Wilhelm, Nature (London) **453**, 1031 (2008).
[2] J. Majer, J. M. Chow, J. M. Gambetta, J. Koch, B. Johnson, J. Schreier, L. Frunzio, D. Schuster, A. Houck, A. Wallraff, A. Blais, M. Devoret, S. Girvin, and R. Schoelkopf, Nature (London) **449**, 443 (2007).
[3] M. Sillanpaa, J. Park, and R. Simmonds, Nature (London) **449**, 438 (2007).
[4] Y. Pashkin, T. Yamamoto, O. Astafiev, Y. Nakamura, D. Averain, and J. Tsai, Nature (London) **421**, 823 (2003).
[5] T. Yamamoto, Y. Pashkin, O. Astafiev, Y. Nakamura, and J. Tsai, Nature (London) **425**, 941 (2003).
[6] P. R. Johnson, F. W. Strauch, A. J. Dragt, R. C. Ramos, C. J. Lobb, J. R. Anderson, and F. C. Wellstood, Phys. Rev. B **67**, 020509(R) (2003).
[7] A. J. Berkley, H. Xu, R. Ramos, M. Gubrud, F. Strauch, P. Johnson, J. Anderson, A. Dragt, C. Lobb, and F. Wellstood, Science **300**, 1548 (2003).
[8] R. McDermott, R. Simmonds, M. Steffen, K. Cooper, K. Cicak, K. Osborn, S. Oh, D. Pappas, and J. Martinis, Science **307**, 1299 (2005).
[9] M. Steffen, M. Ansmann, R. Bialczak, N. Katz, E. Lucero, R. McDermott, M. Neeley, E. Weig, A. Cleland, and J. Martinis, Science **313**, 1423 (2006).
[10] A. O. Niskanen, Y. Nakamura, and J. S. Tsai, Phys. Rev. B **73**, 094506 (2006).
[11] D. V. Averin and C. Bruder, Phys. Rev. Lett. **91**, 057003 (2003).
[12] B. L. T. Plourde, J. Zhang, K. B. Whaley, F. K. Wilhelm, T. L. Robertson, T. Hime, S. Linzen, P. A. Reichardt, C. E. Wu, and J. Clarke, Phys. Rev. B **70**, 140501(R) (2004).
[13] M. Wallquist, J. Lantz, V. Shumeiko, and G. Wendin, New J. Phys. **7**, 178 (2005).
[14] A. van den Brink, A. Berkley, and M. Yalowsky, New J. Phys. **7**, 230 (2005).
[15] A. Fay, E. Hoskinson, F. Lecocq, L. P. Levy, F. W. J. Hekking, W. Guichard, and O. Buisson, Phys. Rev. Lett. **100**, 187003 (2008).
[16] A. Niskansen, K. Harrabi, F. Yoshihara, Y. Nakamura, S. Lloyd, and J. Tsai, Science **316**, 723 (2007).
[17] T. Hime, P. Reichardt, B. Plourde, T. Robertson, C. Wu, A. Ustinov, and J. Clarke, Science **314**, 1427 (2006).
[18] S. H. W. van der Ploeg, A. Izmalkov, A. M. van den Brink, U. Hubner, M. Grajcar, E. Il'ichev, H. G. Meyer, and A. M. Zagoskin, Phys. Rev. Lett. **98**, 057004 (2007).
[19] R. Harris, A. J. Berkely, M. W. Johnson, P. Bunyk, S. Govorkov, M. C. Thom, S. Uchaikin, A. B. Wilson, J. Chung, E. Holtham, J. D. Biamonte, A. Y. Smirnov, M. H. S. Amin, and A. M. van den Brink, Phys. Rev. Lett. **98**, 177001 (2007).
[20] K. Cicak, D. Li, J. A. Strong, M. S. Allman, F. Altomare, A. J. Sirois, J. D. Whittaker, J. D. Teufel, and R. W. Simmonds, Appl. Phys. Lett. **96**, 093502 (2010).
[21] R. W. Simmonds, K. M. Lang, D. A. Hite, S. Nam, D. P. Pappas, and J. M. Martinis, Phys. Rev. Lett. **93**, 077003 (2004).
[22] K. B. Cooper, M. Steffen, R. McDermott, R. W. Simmonds, S. Oh, D. A. Hite, D. P. Pappas, and J. M. Martinis, Phys. Rev. Lett. **93**, 180401 (2004).
[23] L. Tian, M. S. Allman, and R. W. Simmonds, New J. Phys. **10**, 115001 (2008).
[24] A. Blais, R. S. Huang, A. Wallraff, S. M. Girvin, and R. J. Schoelkopf, Phys. Rev. A **69**, 062320 (2004).
[25] S. Haroche and J.-M. Raimond, *Exploring the Quantum* (Oxford University Press, New York, 2006).
[26] S. Ashhab, A. Niskanen, K. Hazrrabi, Y. Nakamura, T. Picot, P. de Groot, C. Harmans, J. Mooij, and F. Nori, Phys. Rev. B **77**, 014510 (2008).
[27] J. M. Martinis, K. B. Cooper, R. McDermott, M. Steffen, M. Ansmann, K. D. Osborn, S. Oh, D. P. Pappas, R. W. Simmonds, and C. C. Yu, Phys. Rev. Lett. **95**, 210503 (2005).
[28] M. S. Allman, F. Altomare, J. D. Whittaker, K. Cicak, D. Li, A. Sirois, J. Strong, J. D. Tuefel, and R. W. Simmonds, arXiv:1004.2738v1.